JOURNAL OF VIROLOGY, Mar. 2004, p. 2956–2966 Vol. 78, No. 6
0022-538X/04/$08.00+0 DOI: 10.1128/JVI.78.6.2956–2966.2004

Influence of Tegument Proteins of Pseudorabies Virus on Neuroinvasion and Transneuronal Spread in the Nervous System of Adult Mice after Intranasal Inoculation

Robert Klopfleisch,[1] Jens P. Teifke,[2] Walter Fuchs,[1] Martina Kopp,[1] Barbara G. Klupp,[1] and Thomas C. Mettenleiter[1]*

Institutes of Molecular Biology[1] and Infectology,[2] Friedrich-Loeffler-Institutes, Federal Research Centre for Virus Diseases of Animals, D-17493 Greifswald-Insel Riems, Germany

Received 5 August 2003/Accepted 19 November 2003

Pseudorabies virus (PrV) is a neurotropic alphaherpesvirus that, after intranasal infection of adult mice, enters peripheral neurons and propagates to the central nervous system. In recent years we have analyzed the contribution of virus-encoded glycoproteins to neuroinvasion and transneuronal spread (reviewed in T. C. Mettenleiter, Virus Res. 92:197–206, 2003). We now extend our studies to analyze the role of tegument proteins in these processes. To this end, PrV mutants unable to express the UL11, UL37, UL46, UL47, and UL48 tegument proteins, as well as the corresponding rescued viruses, were intranasally instilled into 6- to 8-week-old CD1 strain mice. First, mean survival times were determined which showed that mice infected with the UL46 deletion mutant succumbed to the disease as early as wild-type PrV-infected animals. Survival times increased in the order: PrV-ΔUL47-, PrV-ΔUL11-, and PrV-ΔUL48-infected animals, a finding which parallels the growth phenotype of these viruses in cell culture. In contrast, none of the PrV-ΔUL37-infected animals died. Upon closer histological examination, all viruses except PrV-ΔUL37 were able to infect the nasal cavity and propagate to first- and second-order neurons as shown by two-color immunofluorescence. However, neuroinvasion was delayed in PrV-ΔUL47, PrV-ΔUL11, and PrV-ΔUL48, a finding that correlated with the extended survival times. Surprisingly, whereas PrV-ΔUL48 and PrV-ΔUL37 replicated to similar titers in cell culture which were ~500-fold lower than those of wild-type virus, after intranasal infection of mice PrV-ΔUL48 was able to infect areas of the brain like wild-type PrV, although only after a considerably longer time period. In contrast, PrV-ΔUL37 was not able to enter neurons and was restricted to the infection of single cells in the nasal respiratory epithelium. Thus, our data demonstrate the importance of herpesviral tegument proteins in neuronal infection and show a different contribution of tegument proteins to the neuroinvasion phenotype of a neurotropic alphaherpesvirus.

Pseudorabies virus (PrV) is an alphaherpesvirus that causes Aujeszky's disease, a severe neurological disorder, in a broad range of mammalian species. The pig is the natural host of PrV since it is the only animal able to survive a productive infection, and latently infected pigs serve as a virus reservoir. After oronasal infection, which is the natural route of PrV entry into the organism, adult pigs usually show only mild clinical signs of respiratory distress or reproductive failure. In contrast, young piglets are very sensitive to virus invasion of the central nervous system (CNS) (36). Pruritus, the hallmark of the syndrome in nonporcine species, is usually not observed in pigs. In contrast to pigs, the course of infection in susceptible nonporcine species is peracute with a high mortality. These species are endstage hosts, i.e., they generally do not shed the virus and are therefore less important in transmission to other species (25, 29, 30, 45, 56, 60).

Since PrV infects a wide range of mammals, resulting in the rapid induction of strong neurological symptoms, the mouse has become a useful model for investigation of neuroinvasion and transneuronal spread of PrV (20, 22, 23, 53). After intranasal inoculation PrV replicates in the respiratory epithelium, and invades the CNS via the trigeminal nerve, as well as by sympathetic and parasympathetic pathways (4). In mice, the olfactory route is normally not involved in PrV neuroinvasion (4). Following the trigeminal pathway, the virus reaches the trigeminal ganglion (TG) by invading free nerve ends of first-order sensory trigeminal neurons (4, 19). Following the central axons of sensory nerve cells, the virus enters the brain stem and infects second-order neurons in afferent trigeminal nuclei, including the spinal trigeminal nucleus (*Nucleus tractus spinalis nervi trigemini*, Sp5) and the principal sensory trigeminal nucleus (*Nucleus sensibilis pontinus nervi trigemini*, Pr5).

Herpesvirus virions consist of four separate morphological entities: the inner nucleoprotein core, the icosahedral capsid, the tegument, and the envelope. Of these components, the tegument is the least understood. It is a proteinaceous layer composed of more than 15 different proteins that surrounds the capsid. Although considered largely unstructured, at least the inner layer of tegument associated with the capsid may indeed exhibit icosahedral symmetry (14, 65). Herpesvirus particles gain their final tegument during secondary envelopment in the cytosol, which involves the assembly of the complex tegument, as well as budding into trans-Golgi vesicles, thereby acquiring the virion envelope with virus-encoded glycopro-

* Corresponding author. Mailing address: Institute of Molecular Biology, Friedrich-Loeffler-Institutes, Federal Research Centre for Virus Diseases of Animals, Boddenblick 5A, D-17493 Greifswald-Insel Riems, Germany. Phone: 49-38351-7250. Fax: 49-38351-7151. E-mail: mettenleiter@rie.bfav.de.

teins. Tegumentation is a complex process that is apparently driven by specific protein-protein interactions with marked redundancy (48). Tegument proteins are important structural virion components since, like the matrix proteins in RNA viruses, they link virion envelope and nucleocapsid. Moreover, they fulfill important roles during initial stages of viral replication since, after entry of infecting virions into target cells, they are released into the infected cell priming cell function for viral replication. For example, the UL41 gene product is involved in virus-induced host cell shutoff (7, 18), whereas the UL48 protein acts as a potent transactivator of viral immediate-early genes (6, 13). The latter activity is modulated in herpes simplex virus type 1 (HSV-1) by the UL46 and UL47 gene products (47).

Structurally, the innermost layer of the tegument is most probably composed of the UL36 protein, the largest protein found in the herpesvirus family. In HSV-1 it could be shown that this protein is directly associated with the pentons, which are formed by the UL19 major capsid protein (52, 65). The UL19 protein also forms the hexons of the capsid. The UL37 protein physically interacts with UL36 (37) and may build the second layer of the tegument, which is important for the addition of other tegument proteins prior to secondary envelopment (37). In its absence, virus titers are decreased ~500-fold and plaque size is reduced, which correlates with an impairment in virion morphogenesis: intracytoplasmic capsids were observed by electron microscopy to form ordered aggregates (38).

The UL46 and UL47 proteins constitute prominent components of the tegument. Although both are not required for productive viral replication, in cell culture UL47 deletion mutants show a 10-fold decrease in viral titers, and intracytoplasmic aggregates of capsids loosely surrounded by tegument proteins were observed. In contrast, deletion of the UL46 gene did not affect viral titers, whereas plaque size was reduced in both mutants to a similar extent (40). Thus, at least the UL47 protein is involved in virion morphogenesis.

The products of the alphaherpesvirus UL48 homologous genes are components of the virion tegument but, besides this structural role, they also function early after entry of virions into target cells by transactivating immediate-early gene expression (6, 7, 13). The HSV-1 UL48 protein has been proposed to interact with viral glycoproteins B (gB), gD, and gH (66) and thus may be involved in mediating interaction between viral envelope and tegumented capsids. In cells infected with UL48 deletion mutants of PrV, unenveloped capsids were found dispersed in the cytoplasm that correlated with ~500-fold-reduced viral titers and a small plaque phenotype (26).

Herpesvirus UL11 homologous proteins are also thought to be involved in secondary envelopment. The HSV-1 (5, 43), varicella-zoster virus (31), and human cytomegalovirus (59) UL11 homologues have been demonstrated to be myristoylated, and the HSV-1 UL11 protein is also palmitoylated (42). These proteins thus have a high membrane affinity and might possess membrane-targeting functions (8, 44, 58). Although nonessential, deletion of UL11 in PrV resulted in a 10-fold decrease in virus titers and a reduction in plaque size (39). Ultrastructurally, two different phenotypes were observed. Intracytoplasmic membranes presumably originating from the Golgi or *trans*-Golgi region were often found distorted, forming tight multistacks. Moreover, secondary envelopment was impaired, and in a fraction of infected cells PrV capsids surrounded by electron-dense tegument material accumulated in the cytosol in sizeable aggregates (39). This indicates that the UL11 protein is involved in a late step in virion morphogenesis just prior to secondary envelopment.

Whereas the UL46, UL47, and UL48 genes are not conserved within the *Herpesviridae* but are present only in alphaherpesviruses, the UL36, UL37, and UL11 genes are conserved throughout the herpesviruses (46).

In contrast to the role of glycoproteins in herpesvirus neuroinvasion, which has been analyzed extensively in the past several years (1, 2, 3, 4, 24, 34, 63), no thorough examination of the role of viral tegument proteins in this process, except for US9 (11, 12), has thus far been performed. Since gE is a major neurovirulence determinant in alphaherpesviruses and has also been implicated to play an important role in virion morphogenesis during secondary envelopment, it seems reasonable to assume that other proteins involved in virion maturation may also influence alphaherpesvirus neurotropism. This is particularly important in the context of recent findings implicating tegument proteins in the separate intra-axonal transport of nucleocapsids and envelopes to the synapse, where virion maturation may take place (50, 55).

To investigate the influence of different tegument proteins on herpesvirus neuroinvasion, we infected CD1 mice intranasally with PrV mutants with deletions of the UL11, UL37, UL46, UL47, and UL48 genes, respectively. To estimate the effect of the mutation on pathogenicity, we compared clinical symptoms and mean time to death (MTD) and assessed, by histopathology, immunohistochemistry, and two-color immunofluorescence, the kinetics of viral spread within the trigeminal circuit and associated trigeminal nuclei.

MATERIALS AND METHODS

Viruses and cells. PrV strain Kaplan (PrV-Ka) (35) was used as the wild-type control. The construction and characterization of PrV-ΔUL11, PrV-ΔUL37, PrV-ΔUL46, PrV-ΔUL47, and PrV-ΔUL48, as well as UL11, UL46, and UL47 rescuants, has been described elsewhere (26, 38, 40) (Fig. 1). Transfections were carried out in rabbit kidney (RK13) cells. Cells were maintained in minimal essential medium supplemented with 5% fetal bovine serum.

Isolation of ΔUL37 and ΔUL48 rescue mutants. To restore UL37 expression in PrV-ΔUL37, purified PrV-ΔUL37 DNA was cotransfected with a plasmid containing a 4,234-bp *Sph*I-*Bst*XI fragment encompassing the UL37 gene by calcium phosphate coprecipitation (28). Resulting virus stocks were titrated on RK13 cells. Since PrV-ΔUL37 expresses green fluorescent protein (GFP) from the UL37 locus, rescuants were identified by the absence of GFP autofluorescence. Single nonfluorescent plaques were picked and purified to homogeneity, and one rescuant, designated PrV-ΔUL37R, was further analyzed. To reinsert the UL48 gene, RK13 cells were transfected with pUC-B1K containing a 3,605-bp *Bam*HI-*Kpn*I fragment encompassing the UL48 gene (26). After 24 h the cells were infected with PrV-ΔUL48. Resulting virus progeny was titrated on RK13 cells. Since deletion of UL48 resulted in a small plaque phenotype, single plaques with a large diameter were picked for isolation of rescued viruses. After two rounds of plaque purification, a single plaque isolate, designated PrV-ΔUL48R, was randomly chosen for further analysis. Expression of the UL37 and UL48 gene products was analyzed by indirect immunofluorescence with monospecific rabbit antisera against the UL37 protein (diluted 1:500 in Tris-buffered saline (TBS; 0.5 M Tris, 1.5 M NaCl) or the UL48 protein (diluted 1:500 in TBS), respectively. Alexa Fluor 488-labeled anti-rabbit immunoglobulin G (Molecular Probes, Eugene, Oreg.) was used as a secondary antibody. Furthermore, Southern blot analysis proved correct reinsertion of the genes, and gene expression of the rescued and the flanking genes was verified by Western blot analysis (data not shown).

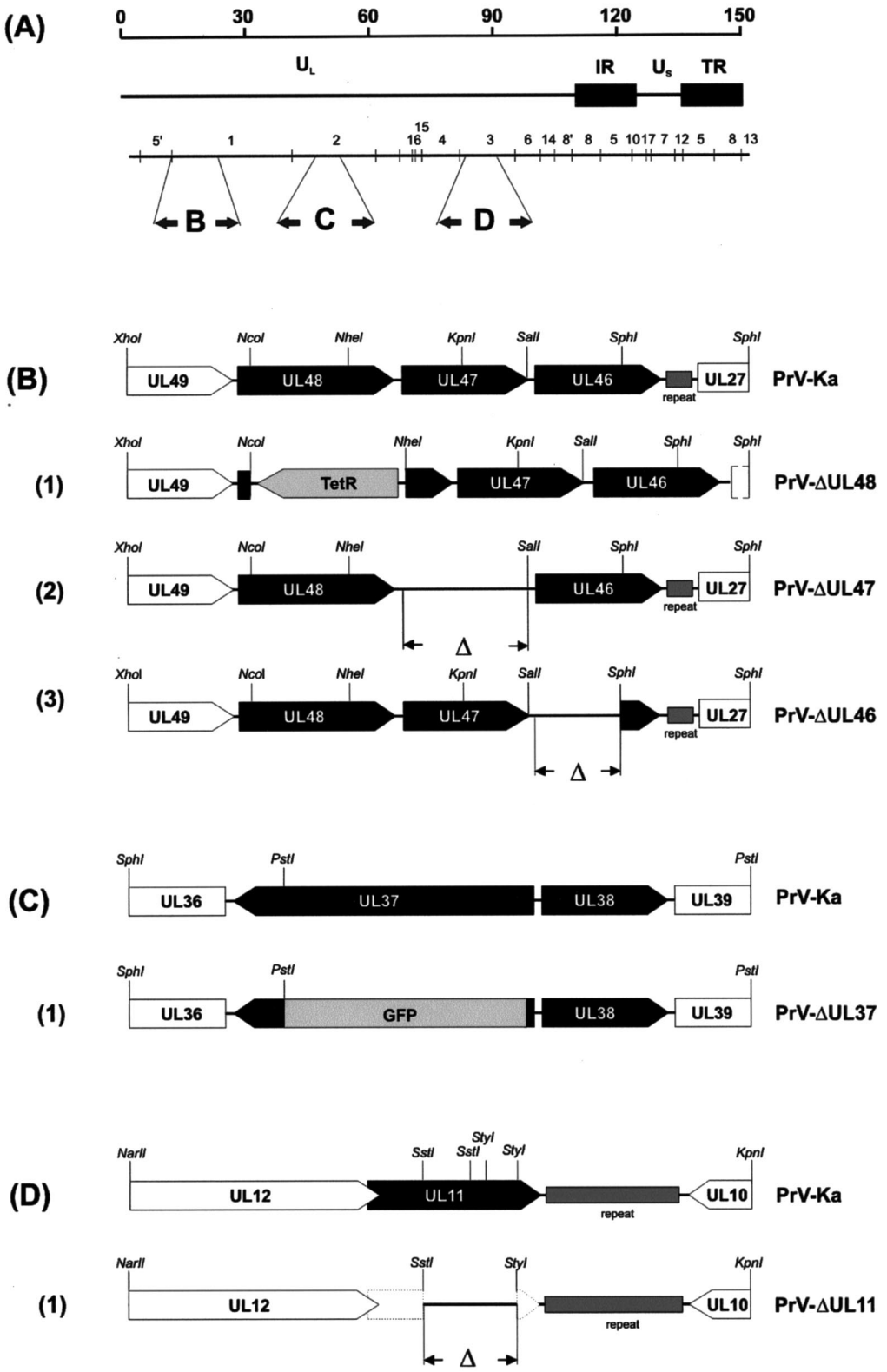

FIG. 1. Genotype of virus mutants. (A) Schematic map of the PrV genome, which consists of a unique long region (U_L) and a unique short region (U_S); the latter is bracketed by inverted repeat sequences (IR and TR). The positions of *Bam*HI restriction fragments and the coding regions of the relevant proteins in the genome are indicated in panels B to D. (B) Enlarged map of the UL46, UL47, and UL48 gene region of *Bam*HI fragment 1. The locations of the open reading frames are shown, and transcriptional orientation is indicated by pointed rectangles. (B1) Deletion mutant PrV-ΔUL48 contains a tetracycline resistance gene (TetR). Deletions in PrV-ΔUL46 (B2) and PrV-ΔUL47 (B3). (C) Enlarged view of the relevant portion of the genome for PrV-ΔUL37. (C1) PrV-ΔUL37 contains a GFP marker cassette. The sequence encoding the GFP insert is not drawn to scale. (D) Enlargement of the PrV UL11 gene region. (D1) Besides deletion of major parts of the UL11 gene, the UL11 start codon was mutated, and a stop codon was generated at amino acid position 3.

Design of animal experiments. For all experiments 6- to 8-week-old mice of the strain CD1 were used. To determine mean survival times, 10 animals for each of the different deletion mutants and PrV-Ka, and 3 animals for each of the rescue mutants were anesthetized with 150 μl of a ketamine (10 mg/ml)-xylazine (1 mg/ml) mixture and infected by bilateral intranasal instillation of 5 μl of the virus suspension containing 10^6 PFU. Whereas PrV-ΔUL37 was propagated on complementing cells prior to infection of mice, the other mutant virus stocks were obtained from noncomplementing cells. Animals were observed twice a day for a period of 14 days or euthanized when severe pruritus developed, followed by excitations and self-mutilation.

To investigate kinetics of infection, three mice for each time point were euthanized sequentially every 24 h after inoculation and subjected to transcardial perfusion with phosphate-buffered saline (150 mM NaCl, 7.4 mM Na_2HPO_4, 2.4 mM KH_2PO_4) for 5 min, followed by 4% paraformaldehyde in phosphate-buffered saline for 10 min by using a peristaltic pump (flow rate, 20 ml/min). After necropsy, the head, including brain and TG, and the spinal cord were fixed for additional 48 h in neutral buffered 4% paraformaldehyde. To investigate the nasal cavity, the skull was decalcified with Formical 2000 (Decal, Tallman, N.Y.) for a further 48 h. For preparation of cryosections, the mice were euthanized, and the brain was dissected. After a short incubation in −70°C *n*-heptane, the tissue was stored at this temperature.

Histopathology and immunohistochemistry. Fixed tissues were embedded in Histosec (Merck, Darmstadt, Germany) and cut at 4 μm in transversal serial sections. The sections were mounted on Super-Frost-Plus glass slides (Menzel-Gläser, Braunschweig, Germany) and stained with hematoxylin-eosin for light microscopy. Immunohistochemistry was performed to detect PrV-antigen in paraffin sections. To this end, a rabbit antiserum specific for the PrV major capsid protein UL19 was used. The avidin-biotin complex (ABC) method was used according to a standardized protocol (33). Briefly, sections were dewaxed and rehydrated, and endogenous peroxidases were blocked with 20 ml of H_2O_2 and 180 ml of methanol for 10 min. After rinsing, an additional blocking step with normal goat serum was performed for 30 min, and sections were incubated with primary anti-UL19 antiserum diluted 1:500 in TBS in a humidity chamber for 1 h. Subsequently, the sections were incubated with a biotinylated goat anti-rabbit immunoglobulin G1 (Vector Laboratories, Burlingame, Calif.; diluted 1:200 in TBS), followed by an incubation with ABC (Vector) diluted 1:10 in TBS for 30 min, providing the conjugated horseradish peroxidase. AEC-Substrate (Dako, Hamburg, Germany) was used as a chromogen. After they were washed in deionized water, sections were counterstained with Mayer's hematoxylin and mounted with Aquatex (Merck). As a control, a commercially available rabbit polyclonal antibody against papillomavirus group-specific antigen was used (Dako). Brains of noninfected mice were used as tissue controls to monitor the specificity of the rabbit anti-UL19 antiserum.

The location (bregma) of the infected nuclei in the brain stem and pons was determined according to the method of Paxinos and Franklin (54).

Immunofluorescence and confocal laser scanning microscopy. Frozen tissues were embedded in tissue freezing medium (Leica Instruments GmbH, Nussloch, Germany), and cut at 5 μm in transversal serial cryosections. The sections were mounted on glass slides (Super-Frost; Menzel-Gläser) and fixed with acetone for 10 min at −20°C.

Two-color immunofluorescence was performed to detect PrV-antigen and neuron-specific nuclear protein (NeuN). For this purpose, rabbit antiserum specific for the PrV major capsid protein UL19 and a mouse anti-NeuN monoclonal antibody (Chemicon, Temecula, Calif.) were used. After a blocking step with 5% bovine serum albumin in TBS for 30 min, sections were incubated with a mix of the primary antibodies (anti-UL19 antiserum diluted 1:500 and anti-NeuN antibody diluted 1:150 in TBS) in a humidity chamber for 1 h. Subsequently, after a thorough wash with TBS, the sections were incubated for 1 h with a mix of fluorescein isothiocyanate (FITC)-labeled swine anti-rabbit immunoglobulin (Dako; diluted 1:400 in TBS) and indocarbocyanine (Cy3)-labeled goat anti-mouse immunoglobulin (Dianova, Hamburg, Germany; diluted 1:800 in TBS). After being washed in TBS, sections were mounted with 25 mg of 1,4-diazabicyclo[2.2.2]-octane (DABCO; Sigma) per ml of glycerol. Nonneuronal tissue of mice was used as control to monitor the specificity of the NeuN antibody. As an irrelevant control, a mouse anti-desmin monoclonal antibody was used (Dako).

For scanning and photography, a LSM510 (Zeiss, Göttingen, Germany) was used. FITC was excited at 488 nm and detected via a 505- to 530-nm band-pass filter. Cy3 was excited at 543 nm and detected with a 585-nm long-pass filter. The pinhole diameters of each detection channel were set at 100 μm. Two-channel frame-by-frame multitracking was used for detection to avoid "cross talk" signals. The different frames were scanned separately, with appropriate installation of the optical path for extinction and emission of each scan according to the manufacturer's instructions.

RESULTS

Kinetics of wild-type PrV infection. The first symptoms after infection with PrV-Ka were observed at 36 h postinfection (p.i.) when mice became anorectic, apathetic, depressed, and cowered in a hunched position. Subsequently, the animals showed frequent attacks characterized by extensive scratching of the skin of the face, nose, and maxillary region, thereby causing severe hemorrhagic dermal erosions and ulcerations with coinciding acute catarrhal conjunctivitis ("mad itch" syndrome). Hyperactivity with excitations and convulsions, heavy dyspnea with tachypnea, and a moderate swelling of the bridge of the snout were also observed. All infected mice died at an average time of 49.5 h p.i. (Table 1). Detection of the PrV major capsid protein encoded by the UL19 gene was used as a marker for virus infection. UL19 antigen was present in ciliated cells of the pseudostratified respiratory epithelium of the nasal mucosa at 24 h p.i. Morphologically, infected cells were slightly to moderately swollen or had indistinct or disrupted cellular borders with karyorrhectic nuclei (degeneration and necrosis). UL19-positive cells were consistently found in small to medium-sized clusters in all parts of the nasal cavity lined with respiratory epithelium (Fig. 2A and 3A). Starting at 24 h p.i., scattered infection of serous glands located within the lamina propria of the nasal respiratory mucosa was observed. Few infected neurons in the TG in two of three mice were detected at 24 h p.i. (Fig. 3B). At 48 h p.i. the number of infected cells in the ganglion was strongly increased (Fig. 2B and 3C).

UL19 antigen could also be detected at 48 h p.i. in the trigeminal nuclei of the pons and the brain stem, corresponding to the time the animals exhibited severe symptoms (Fig. 3D). The caudal part of the spinal trigeminal nucleus (Sp5, bregma −5.68 to −8.24) and the spinal trigeminal tract nucleus (Sp5T, bregma −5.4 to −8.24) were mainly affected by the viral infection, as determined by anti-UL19 immunohistochemistry (Fig. 2C). As shown by confocal laser scanning microscopy UL19 antigen was present in NeuN-antigen positive second-order neurons of the Sp5 (Fig. 4A). Similar signals were also detectable in the Pr5.

Deletion of the UL46 or UL47 genes does not significantly alter neuroinvasion of PrV. The pathogenicity of PrV-ΔUL46 was very similar to PrV-Ka. First clinical signs of a PrV infection could be seen at 36 h p.i. At this time, mice started to be depressed and anorectic and exhibited a hunched position. In the following hours the animals became severely pruritic and started to scratch their head excessively, leading to subsequent profound dermal lesions and conjunctivitis. Intermittent convulsions with dyspnea were also observed, and swelling of the bridge of the snout occurred. The animals died at an average time of 50.5 h p.i. (Table 1). Immunohistochemistry revealed a staining pattern similar to that of PrV-Ka-infected animals. UL19-positive cells could be detected in the nasal respiratory epithelium at 24 h p.i. (Fig. 3A). They formed multiple clusters of necrotic cells distributed in the respiratory mucosa. Starting at 48 h p.i., scattered serous glands were also UL19-antigen positive. At 24 h p.i. a few perikarya of the TG were infected exhibiting strong intracytoplasmic and intranuclear staining (Fig. 3B). At 48 h p.i., the number of infected cells in the TG was considerably increased (Fig. 3C). As in PrV-Ka-infected

TABLE 1. MTD, clinical symptoms, and appearance of PrV antigen-positive cells in mice infected experimentally with PrV-Ka and PrV mutants with deletions of different tegument protein genes

Parameter	Result with virus:					
	PrV-Ka	PrV-ΔUL46	PrV-ΔUL47	PrV-ΔUL11	PrV-ΔUL48	PrV-ΔUL37
MTD[a] (SD) in h (n = 10)	49.5	50.5 (1.69)	56.5 (1.80)	67 (1.58)	126.75 (1.93)	>240
Clinical symptoms[b] at:						
24 h p.i.	0	0	0	0	0	0
48 h p.i.	+++	+++	+++	+	0	0
65 h p.i.	†	†	†	+++	+	0
96 h p.i.	†	†	†	†	++	0
120 h p.i.	†	†	†	†	+++	0
Immunohistochemistry[c] at:						
24 h p.i.						
Nasal cavity	+	+	+	+	+	+
First-order neurons	+	+	−	−	−	−
Second-order neurons	−	−	−	−	−	−
48 h p.i.						
Nasal cavity	+	+	+	+	+	+
First-order neurons	+	+	+	+	−	−
Second-order neurons	+	+	+	−	−	−
65 h p.i.						
Nasal cavity				+	+	+
First-order neurons	†	†	†	+	+	−
Second-order neurons				+	−	−
96 h p.i.						
Nasal cavity					+	+
First-order neurons	†	†	†	†	+	−
Second-order neurons					+	−
120 h p.i.						
Nasal cavity					+	−
First-order neurons	†	†	†	†	+	−
Second-order neurons					+	−

[a] An average was calculated for 10 animals in each group. Standard deviation is indicated in parentheses.
[b] Clinical symptoms: 0, clinically normal mice; +, slight depression, hunched position, ruffled hair coat; ++, apathy, anorexia, moderate dyspnea, slight facial pruritus; +++, severe attacks of excitation, self-mutilation, skin erosions, heavy dyspnea; †, animals moribund or dead.
[c] Immunohistochemistry: +, UL19 antigen detectable; −, UL19 antigen not detectable; †, animals moribund or dead. Nasal cavity, respiratory mucosal epithelium; first-order neurons, TG; second-order neurons, spinal trigeminal nucleus (Sp5), spinal trigeminal tract nucleus (Sp5T), mesencephalic trigeminal nucleus (Me5), and principal sensory trigeminal nucleus (Pr5).

animals, UL19 protein was present in the first-order trigeminal nuclei at 48 h p.i. when the animals reached the clinically fulminant stage of the disease. Again, Sp5 was the location in the CNS that was mainly affected (Fig. 3D). In Pr5 only a few cells were positive for PrV antigen.

After infection with PrV-ΔUL47 the animals survived somewhat longer, with a mean survival time of 56.5 h p.i., while the onset and the intensity of symptoms as well as the numbers and locations of infected cells in the peripheral nervous system and CNS were similar to those of mice infected with PrV-Ka or PrV-ΔUL46 (Table 1). However, the animals showed an ~8 h longer initial phase of depression and hunching. Once the animals had started with scratching, excitation attacks, and progressive dyspnea, the overall condition deteriorated in the same time frame as observed in animals infected with PrV-Ka.

Clusters of infected and focally necrotic cells of the respiratory epithelium in the nasal cavity were detected at all time points investigated (24, 48, and 56 h p.i.) (Fig. 3A and data not shown). Single glandular epithelial cells were infected at 48 h p.i. Within the TG no infected cells were present at 24 h p.i. (Fig. 3B), but strong PrV-specific signals were observed at 48 h p.i (Fig. 3C). At 56 h p.i., Sp5 and Pr5 were infected to an extent similar to infection with PrV-Ka (Fig. 3D). UL19 antigen and NeuN antigen were clearly demonstrated within the same neuronal cells in the Sp5 (Fig. 4B and C), thus proving that the infected cells were indeed neurons.

Deletion of UL11 and UL48 results in a prolonged MTD and delayed viral spread to second-order neurons. After infection with PrV-ΔUL11, a considerably prolonged MTD of 67 h was observed (Table 1). The first clinical symptoms occurred at 48 h p.i. when animals started to have slightly reduced activity and were anorectic. In the following 12 h they developed severe respiratory distress and cowered in a hunched position. At 60 h p.i. all mice became excited and hyperactive and showed attacks of scratching the facial skin. Thus, the sequence and the intensity of symptoms of the clinical course were comparable

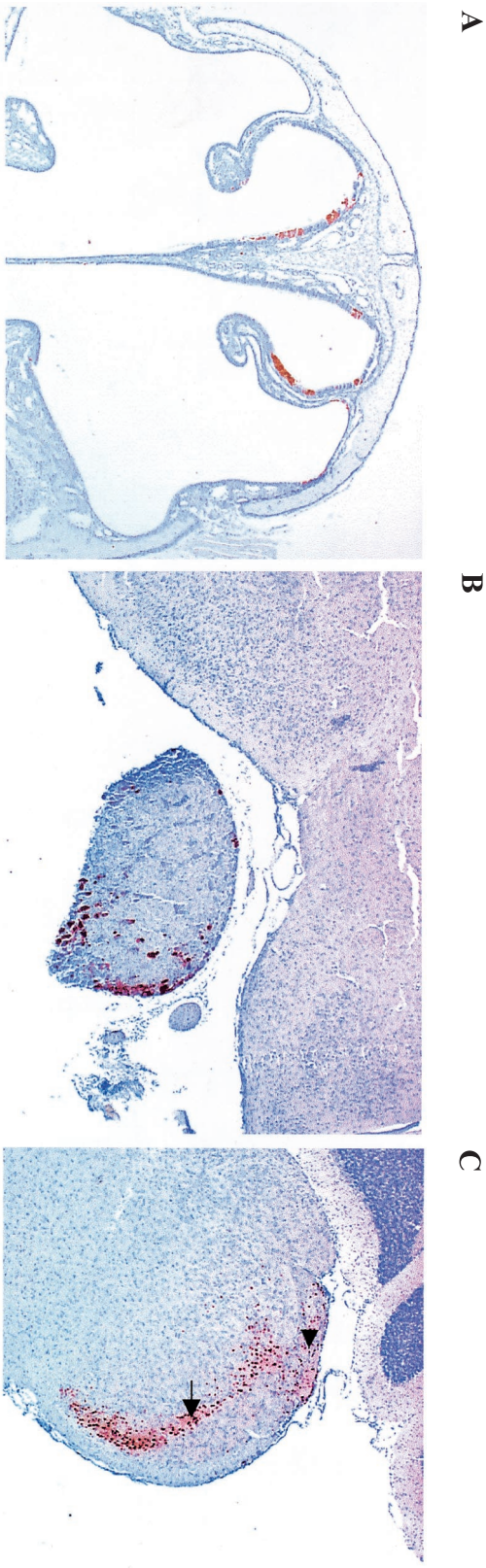

FIG. 2. Immunohistochemistry for detection of PrV-antigen in mice after inoculation with PrV-Ka. Mice were infected in both nostrils with 10^6 PFU. Nose, TG, and brain stem samples were collected from mice sacrificed at the terminal stage of disease at 49.5 h p.i. Immunostaining was performed with an antiserum specific for the PrV major capsid protein. (A) Rostral part of the nasal cavity showing infected cells of the respiratory epithelium on both sides of the nasal septum and dorsal conchae. Magnification, ×25. (B) TG and the basis of the midbrain showing numerous ganglion cells with strong intracytoplasmic and intranuclear staining. Magnification, ×30. (C) Medulla oblongata (bregma −7.00) showing infection of neurons and glial cells of the spinal trigeminal nucleus (Sp5; arrow) and the spinal trigeminal tract (Sp5T, arrowhead). Magnification, ×30.

to the situation after infection with PrV-Ka but started later and showed a delayed progression. Immunostaining in the nasal respiratory epithelium showed positive cells at 24 h p.i. comparable to PrV-Ka infection (Fig. 3A). After 48 h p.i., cells of serous glands were also infected. PrV antigen in neurons was first detectable at 48 h p.i. in an intense staining pattern in a large number of neurons in the TG (Fig. 3C). After 48 h, a small number of axons in the trigeminal roots entering the brain stem carried viral antigen, but none of the second-order neurons were positive at this time point, a finding that is in contrast to those for previously described mutants (Fig. 3D). At 65 h p.i., cells in Sp5 and, to a lesser extent, in Pr5 exhibited viral antigen (Fig. 3F) which were identified as neurons by the presence of NeuN antigen (Fig. 4D).

Infection with PrV-ΔUL48 resulted in death after an average of 126.75 h p.i. (Table 1). The incubation time was also significantly prolonged compared to infection with PrV-Ka. Weak clinical signs of depression and ruffled hair were first observed at 72 h p.i. At 96 h p.i., the animals were severely apathetic and anorectic; at 120 h p.i., they developed the "mad-itch" syndrome with excitations, hyperactivity, and self-mutilation. Clusters of infected cells in the respiratory mucosa of the nasal cavity were observed at all time points from 24 h p.i. onward (Fig. 3A). However, the number of UL19 antigen-positive cells increased with time. From 72 h p.i. infection of glandular epithelium was also observed. At that time only a few infected cells were observed in the TG (Fig. 3E). At 96 and 120 h p.i., the fractions of infected TG neurons increased to levels obtained in an infection with PrV-Ka (Fig. 3G).

Whereas at 96 h p.i. only a few infected cells in the Sp5 were found, after 120 and 126 h p.i. neurons in Sp5 and Pr5 showed an intense staining for UL19 antigen (Fig. 3H). Colocalization of UL19 antigen with the NeuN antigen in the Sp5 at 120 h p.i. again verified that second-order neurons were infected (Fig. 4D). Together, these data indicate that entry into neurons and transneuronal spread was significantly impaired in PrV-ΔUL48, whereas entry into primary target cells in the nasal epithelium was not inhibited.

The presence of UL37 is crucial for PrV neuroinvasion. Of the tested tegument protein mutants, PrV-ΔUL37 showed the strongest defect in neuroinfectivity. Until the termination of the experiment after 240 h p.i., none of the mice developed any symptoms of a PrV infection (Table 1). At days 1 and 2 p.i. in two of three mice and at days 3 and 4 in one of three mice, only a few cells stained positive for UL19 antigen in the respiratory epithelium of the nasal cavity, despite the fact that infection occurred in this case with phenotypically complemented virus (Fig. 3A). No serous glands were found to be positive for UL19 antigen. Furthermore, no viral antigen was found at any time point in the TG, Sp5, or Pr5 (Fig. 3A to H).

Rescue of viral gene expression restores the virulent wild-type phenotype. Restoration of expression of the deleted viral genes in PrV-ΔUL11R, PrV-ΔUL47R, PrV-ΔUL48R, and PrV-ΔUL37R in all cases resulted in a repair of the observed phenotype. After intranasal infection of mice with the rescued viruses, wild-type-like survival times and equivalent progress of disease was observed (data not shown). This finding indicates that the observed phenotypes in vivo were due to the absence of the respective tegument protein.

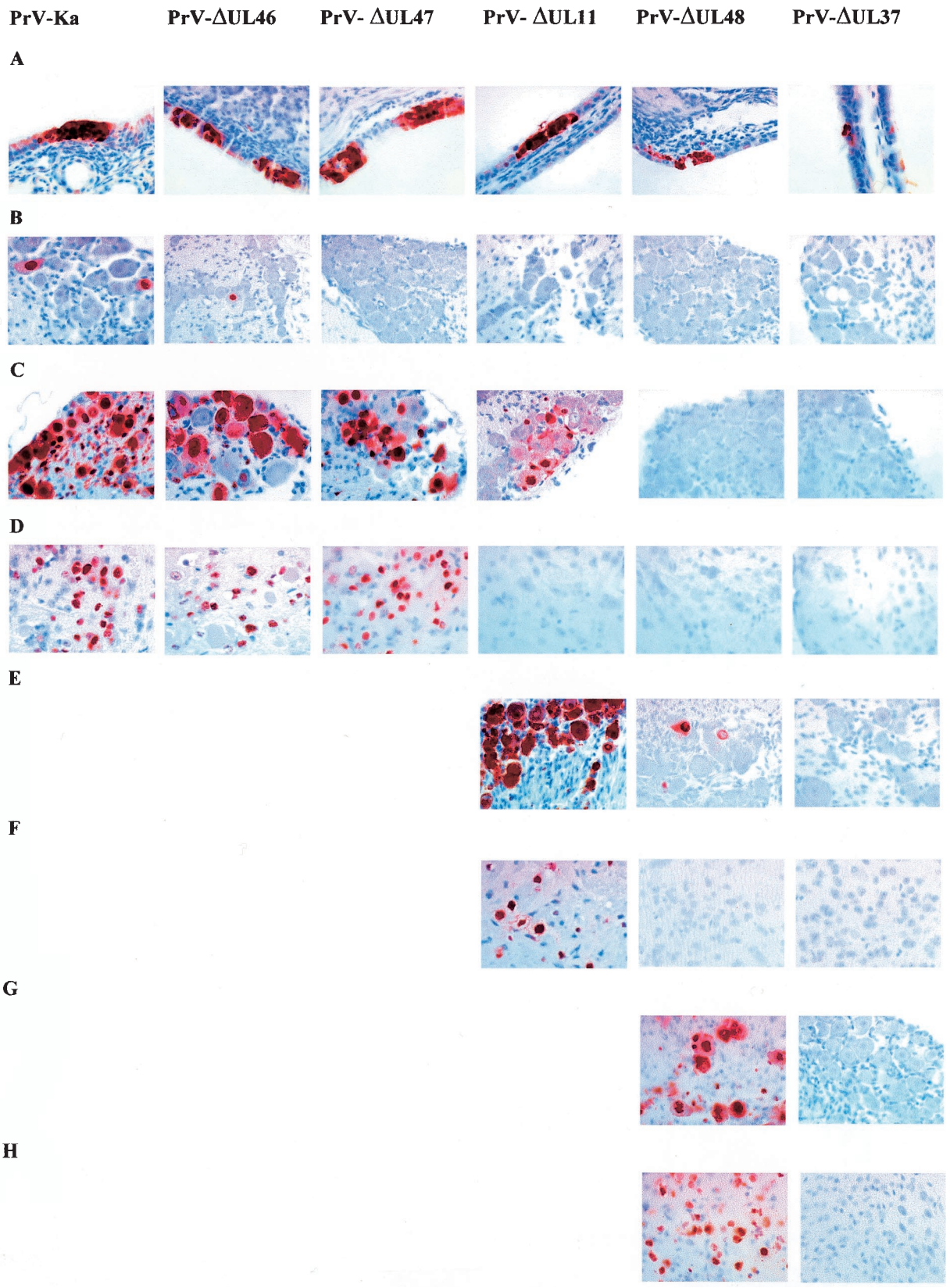

FIG. 3. Immunohistochemistry for detection of PrV-antigen in mice experimentally infected with PrV-Ka or with PrV-ΔUL46, PrV-ΔUL47, PrV-ΔUL11, PrV-ΔUL48, or PrV-ΔUL37. Mice were infected in both nostrils with 10^6 PFU of each virus. Nose, TG, and brain stem samples were collected from mice sacrificed at the different time points. Immunostaining was performed with an antiserum specific for the PrV major capsid

DISCUSSION

In the past, the role of virus-encoded glycoproteins in neuroinvasion and transneuronal spread of PrV has been analyzed extensively (reviewed in reference 49). It has been shown that glycoproteins necessary for entry into cultured cells are also required for entry into neuronal and nonneuronal target cells in the animal and that glycoproteins dispensable for in vitro replication are generally also dispensable for replication in vivo. However, the nonessential gE has been described as a specific neurovirulence determinant in PrV that is required for transneuronal transfer of virus infection in at least some neuronal circuits (21). gE has also been shown to be involved in virion formation in the cytoplasm, presumably by interacting with viral tegument proteins (9, 10, 27). The herpesvirus tegument is composed of more than 15 different virus-encoded proteins which, during tegumentation, apparently interact in a highly intricate network (48).

Recent publications have shown the implications of deletions in the PrV UL11, UL37, UL46, UL47, and UL48 genes, which all encode tegument proteins, on virion formation in cell culture (26, 38, 39, 40). Here, we tested these mutants for their in vivo phenotype after intranasal infection of mice. Generally, the neuroinvasion phenotype in vivo largely reflects the growth pattern in vitro. However, despite differences in impairment of cell-to-cell spread in vitro, all mutants except PrV-ΔUL37 were capable of transneuronal spread and infected second-order neurons.

Mutants lacking UL46 or UL47 genes exhibited only a slight delay in neuroinvasion with no difference in the extent of replication in the nasal epithelium. This again correlates with the in vitro replication since a virus mutant lacking UL46 showed only a slight reduction in plaque size with unaltered final virus titers compared to wild-type PrV. A mutant lacking UL47 demonstrated a similar reduction in plaque size but, in addition, an ~10-fold reduction in virus titers (40). With regard to the MTD, PrV-ΔUL46 was similar to wild-type PrV, whereas the MTD in PrV-ΔUL47-infected animals was slightly longer. No major differences in the extent and kinetics of infection in the nasal cavity or in first- or second-order neurons were observed.

In contrast, in PrV-ΔUL11-infected cultured cells secondary envelopment was inhibited to a larger extent, and distortions of intracytoplasmic membranes in addition to clusters of tegumented capsids in the cytosol were observed, although virus titers were only reduced ~10-fold (39). After intranasal infection of mice, the MTD was longer than in animals infected by PrV-ΔUL46 or PrV-ΔUL47, and a delay in the occurrence of clinical symptoms, as well as in neuroinvasion, was observed. Although we are currently unable to unequivocally prove a causal link between the in vivo and in vitro phenotypes, we consider it likely that the defect in neuroinvasion is caused by a defect in virion maturation. Clearly, the defect is linked to UL11 since restoration of UL11 expression resulted in wild-type-like growth properties in cell culture (39) and in the animal host (the present study).

After infection with PrV-ΔUL48, virus-infected cells in the nasal mucosa were observed similar to all other virus mutants analyzed. However, clinical symptoms, as well as infected neurons, did not appear before 65 h p.i., at a time when animals infected with the UL46, UL47, and UL11 deletion mutants were severely ill or already dead. From the first occurrence of infected neurons until death of the animals, another ~60-h period elapsed. Thus, PrV-ΔUL48 had a severe defect in entering or replicating in first-order neurons. Moreover, subsequent neuronal spread was delayed reflected by an extended course of disease. In cell culture, the UL48 gene products of alphaherpesviruses have been shown to serve a dual function. They represent important constituents of the tegument, and in their absence tegumentation is severely impaired (26, 51). In addition, during entry they are relased into the cytosol, reach the nucleus, and transactivate viral immediate-early genes (6). Whereas both functions are important, it has been shown that deletion of UL48 in PrV more severely affected later than earlier steps in viral replication (26). Thus, although a contribution of the lack of immediate-early transactivation to the observed in vivo phenotype cannot be excluded, it is reasonable to assume that the role of UL48 in morphogenesis is largely responsible for the observed defect. Whether this effect is direct or indirect is unclear. The HSV-1 UL48 protein interacts with the UL41 protein during tegumentation (61) and, in the absence of the UL48 protein, incorporation of the UL41 protein is also impaired (41, 57). Although this interaction has not been described between the corresponding PrV homologues, we cannot exclude that the observed phenotype in vivo is also influenced by a lack of UL41.

Although deletions of UL48 or UL37 from the PrV genome produced virus mutants with similar reduced growth properties in cell culture and a strong reduction in plaque size (26, 38), the in vivo phenotype differed. Even after infection with phenotypically complemented PrV-ΔUL37 neuronal infection was blocked, and no PrV-infected neurons could be detected. However, replication in the primary target cells in the nasal epithelium apparently was also inhibited since very few infected cells were observed in the mucosa, although mice were

protein. Magnification, ×100. (A) Nasal respiratory mucosa at 24 h p.i. showing clusters of infected epithelial cells with strong intracytoplasmic and intranuclear immunostaining. Note the small foci of cells infected with PrV-ΔUL37. (B) TG at 24 h p.i. Only mice infected with PrV-Ka and PrV-ΔUL46 showed a very small number of PrV antigen positive cells at this time point. (C) TG at 48 h p.i. Animals infected with PrV-Ka, PrV-ΔUL46, or PrV-ΔUL47 show a large number of infected cells. In PrV-ΔUL11-infected mice, only a few neurons are infected at this time point. (D) Spinal trigeminal nucleus at 48 h p.i. (56 h p.i. for ΔUL47). Animals infected with PrV-Ka, PrV-ΔUL46, or PrV-ΔUL47 exhibited numerous infected neurons, whereas no infection was detectable in PrV-ΔUL11-, PrV-ΔUL48-, or PrV-ΔUL37-infected mice. (E) TG at 65 h p.i. showing strong infection in mice inoculated with PrV-ΔUL11. Only a few positive ganglion cells could be seen in mice infected with PrV-ΔUL48. (F) Spinal trigeminal nucleus at 65 h p.i. showing strong staining in numerous neurons after PrV-ΔUL11 infection and no staining after PrV-ΔUL48 or PrV-ΔUL37 infection. (G) TG at 120 h p.i. showing an increased number of antigen-positive neurons in mice infected with PrV-ΔUL48 and no antigen detectable in mice infected with PrV-ΔUL37. (H) Spinal trigeminal nucleus at 120 h p.i. showing severe infection with PrV-ΔUL48 and no antigen detectable after inoculation with PrV-ΔUL37.

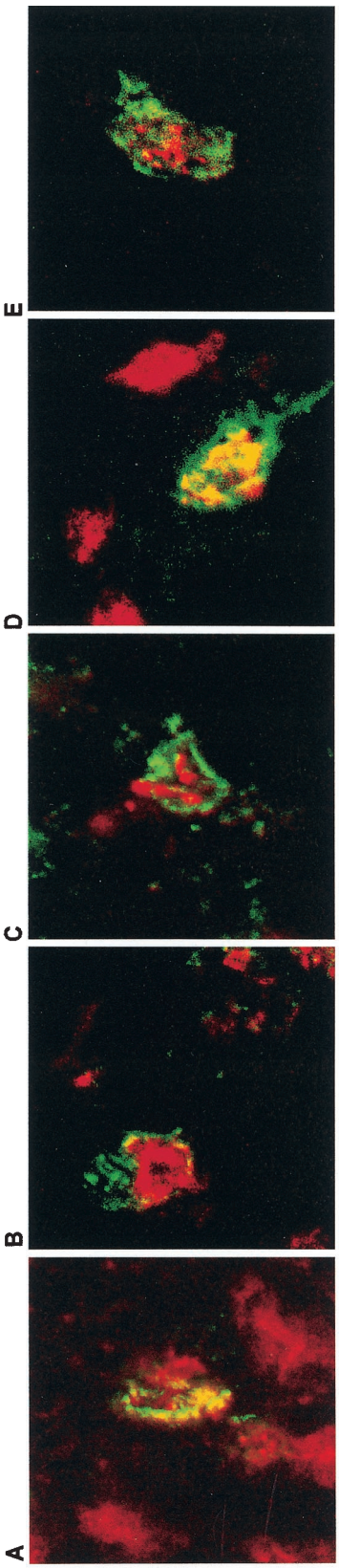

FIG. 4. Two-color immunofluorescence for detection of PrV-antigen and neuron-specific nuclear protein (NeuN) in the Sp5 after inoculation of mice with 10^6 PFU of PrV-Ka (A) and of the mutants PrV-ΔUL46 (B), PrV-ΔUL47 (C), PrV-ΔUL11 (D), or PrV-ΔUL48 (E). Brain samples were collected from mice sacrificed at the terminal stage of disease. Detection of the PrV major capsid protein corresponds to green FITC fluorescence, and detection of NeuN corresponds to red Cy3 fluorescence. Magnification, ×300.

infected with an infectious dose like that used with the other mutant viruses. This result is best explained by the severe defect of PrV-ΔUL37 in direct cell-to-cell spread, which seems to be the major mechanism of viral spread once infection of primary target cells occurred (2, 32). Thus, PrV-ΔUL48 is able to spread quite efficiently in the nasal epithelium, which increases the chance for infection of nerve endings in the mucosa, whereas PrV-ΔUL37 is not. The latter phenotype is linked to the absence of the UL37 gene since restoration of UL37 expression rescued neuroinvasion and neurovirulence. In cell culture, in the absence of UL37, intracytoplasmic clusters of apparently naked capsids form in a regular order (38). The failure of PrV-ΔUL37 to propagate in the nasal mucosa may be linked to this phenotype. Unfortunately, electron microscopic examinations of tissue samples to verify this phenotype in vivo are unrealistic due to the very low number of PrV-ΔUL37-infected cells in the nasal mucosa.

It is interesting that only the PrV mutant lacking UL37 was unable to enter the nervous system after intranasal infection of mice. The UL37 protein was proposed to constitute the inner layer of tegument interacting with capsid-associated UL36 tegument protein (37, 65). Both proteins are conserved within the *Herpesviridae*. Whereas deletion of UL36 resulted in a lethal phenotype in vitro in PrV (B. G. Klupp and W. Fuchs, unpublished results) and HSV-1 (16), deletion of PrV UL37 led to ~500-fold-reduced titers and a drastic reduction in plaque size, but mutant virus was still able to propagate on noncomplementing cells. In HSV-1, a UL37 deletion mutant proved to be replication competent only on complementing cells (15). In our intransal infection model, PrV was not able to infect neurons without UL37. However, it is unclear whether this is due to a defect in replication in nonneuronal cells, thereby limiting the amount of progeny virus available for infection of neurons as secondary target cells, whether cell-to-cell spread from primary infected epithelial cells to neighboring epithelial and nonepithelial cells is impaired, or whether this is a specific neuron-related phenomenon with defects in either entry into or replication in neuronal cells. In any case, of the five tested tegument proteins, UL37 proved to be the most important factor for causing disease.

It is generally assumed that direct infection of neurons in the nasal cavity after intranasal installation is a rare event and that efficient primary replication in epithelial cells is required for efficient neuronal infection (4). This might be due to the morphological structure of the nasal mucosa. The nasal respiratory epithelium consists of a pseudostratified columnar ciliated epithelium, supported by a vascular lamina propria containing serous and mucous glands. The maxillary branch of the trigeminal nerve innervates this epithelium by free nerve endings. Free nerve endings, the simplest form of sensory receptors, are numerous under the epithelium and found mainly along the border between epithelium and lamina propria. This implies a requirement for the virus to penetrate or lyse the epithelium to infect neuronal tissue in the nose. Thus, a defect in cell-to-cell spread of the PrV-ΔUL37 mutant would block neuronal infection indirectly.

In infected neurons herpesviruses replicate in the nucleus but for transneuronal spread viral subassemblies, i.e., tegumented capsids and envelope glycoprotein-containing vesicles are transported separately in the axon (55). The formation of

complete virions is then thought to occur at the synapse, if at all (21, 65). This parallels virion maturation in the cytoplasm of infected tissue culture cells (48). The main difference between the situation in cultured cells and in neurons in vivo is that in the latter fast intra-axonal transport of the viral subassemblies occurs over long distances. Thus far, it is unclear which viral proteins interact with the cellular microtubule-associated transport machinery for long-distance transport to the synapse (21). Although our studies do not directly address this issue, it is clear from our experiments that at least the UL46 and UL47 proteins, which are major tegument components, are not required for this process. Moreover, PrV-ΔUL11, though delayed, also reaches higher areas of the brain quite efficiently, indicating that it cannot be exclusively responsible for interaction of viral cargo with the cellular transport system.

After infection with PrV-ΔUL48, although there was a long delay in the induction of symptoms and a protracted course of disease thereafter, finally at 120 h p.i. all neuronal centers were infected to a similar extent as in wild-type-PrV-infected animals after 48 h. Apparently, the kinetics of infection is different in PrV-ΔUL48 and not the principal ability of the virus to infect certain neuronal cells. Since all mutant virus-infected animals with the exception of PrV-ΔUL37 succumbed to the disease, all mutant viruses except PrV-ΔUL37 must have reached and destroyed cells important for survival of the animals. At present, the underlying mechanism of peracute death due to PrV infection is unknown. It has been assumed that death may be caused by respiratory paralysis (17) or sympathetic disorder (62). Our observations confirm an extensive infection of the superior cervical ganglion at late stages of infection. Moreover, the extensive PrV infection in the nucleus of the solitary tract is noteworthy (data not shown). These neuronal cell bodies in the dorsomedial brain stem are innervated by axons of first-order cells whose cell bodies are located in sensory ganglia of the V, VII, IX, and X nerves. In addition, we observed an infection of the parasympathetic pterygopalatine ganglion, which contains mainly afferent parasympathetic first-order neurons. However, despite heavy infection of these areas in animals infected with gE-null mutants of PrV they still live significantly longer than wild-type PrV-infected animals (64). Thus, the reason for the ultimate death of the infected animals has still to be elucidated at the histological level.

ACKNOWLEDGMENTS

We thank Christian Wetzel and Nils Damann for help in establishing the perfusion technique; Matthias Lenk for excellent support with the laser scanning microscopy; Gabriele Czerwinski, Charlotte Ehrlich, Uta Hartwig, and Nadine Müller for excellent technical assistance; and Elke Zorn for photographic help.

This study was supported by a grant from the Deutsche Forschungsgemeinschaft (Me 854/6-1).

REFERENCES

1. **Babic, N., B. Klupp, A. Brack, T. C. Mettenleiter, G. Ugolini, and A. Flamand.** 1996. Deletion of glycoprotein gE reduces the propagation of pseudorabies virus in the nervous system of mice after intranasal inoculation. Virology **219:**279–284.
2. **Babic, N., B. G. Klupp, B. Makoschey, A. Karger, A. Flamand, and T. C. Mettenleiter.** 1996. Glycoprotein gH of pseudorabies virus is essential for penetration and propagation in cell culture and in the nervous system of mice. J. Gen. Virol. **77:**2277–2285.
3. **Babic, N., T. C. Mettenleiter, A. Flamand, and G. Ugolini.** 1993. Role of essential glycoproteins gII and gp50 in transneuronal transfer of pseudorabies virus from the hypoglossal nerves of mice. J. Virol. **67:**4421–4426.
4. **Babic, N., T. C. Mettenleiter, G. Ugolini, A. Flamand, and P. Coulon.** 1994. Propagation of pseudorabies virus in the nervous system of the mouse after intranasal inoculation. Virology **204:**616–625.
5. **Baines, J., and B. Roizman.** 1992. The UL11 gene of herpes simplex virus 1 encodes a function that facilitates nucleocapsid envelopment and egress from cells. J. Virol. **66:**5168–5174.
6. **Batterson, W., and B. Roizman.** 1983. Characterization of the herpes simplex virion-associated factor responsible for the induction of alpha genes. J. Virol. **46:**371–377.
7. **Berthomme, H., B. Jacquemont, and A. Epstein.** 1993. The pseudorabies virus host-shutoff homolog gene: nucleotide sequence and comparison with alphaherpesvirus protein counterparts. Virology **193:**1028–1032.
8. **Bowzard, J. B., R. J. Visalli, C. B. Wilson, J. S. Loomis, E. M. Callahan, R. J. Courtney, and J. W. Wills.** 2000. Membrane targeting properties of a herpesvirus tegument protein-retrovirus Gag chimera. J. Virol. **74:**8692–8699.
9. **Brack, A. R., J. M. Dijkstra, H. Granzow, B. G. Klupp, and T. C. Mettenleiter.** 1999. Inhibition of virion maturation by simultaneous deletion of glycoproteins E, I, and M of pseudorabies virus. J. Virol. **73:**5364–5372.
10. **Brack, A. R., B. G. Klupp, H. Granzow, R. Tirabassi, L. W. Enquist, and T. C. Mettenleiter.** 2000. Role of the cytoplasmic tail of pseudorabies virus glycoprotein E in virion formation. J. Virol. **74:**4004–4016.
11. **Brideau, A. D., J. P. Card, and L. W. Enquist.** 2000. Role of pseudorabies virus Us9, a type II membrane protein, in infection of tissue culture cells and the rat nervous system. J. Virol. **74:**834–845.
12. **Brideau, A. D., M. G. Eldridge, and L. W. Enquist.** 2000. Directional transneuronal infection by pseudorabies virus is dependent on an acidic internalization motif in the Us9 cytoplasmic tail. J. Virol. **74:**4549–4561.
13. **Campbell, M. E., J. W. Palfreyman, and C. M. Preston.** 1984. Identification of herpes simplex virus DNA sequences which encode a *trans*-acting polypeptide responsible for stimulation of immediate-early transcription. J. Mol. Biol. **180:**1–19.
14. **Chen, D. H., H. Jiang, M. Lee, F. Liu, and Z. H. Zhou.** 1999. Three-dimensional visualization of tegument/capsid interactions in the intact human cytomegalovirus. Virology **260:**10–16.
15. **Desai, P., G. L. Sexton, J. M. McCaffery, and S. Person.** 2001. A null mutation in the gene encoding the herpes simplex virus type 1 UL37 polypeptide abrogates virus maturation. J. Virol. **75:**10259–10271.
16. **Desai, P. J.** 2000. A null mutation in the UL36 gene of herpes simplex virus type 1 results in accumulation of unenveloped DNA-filled capsids in the cytoplasm of infected cells. J. Virol. **74:**11608–11618.
17. **Dolivo, M., E. Beretta, V. Bonifas, and C. Foroglou.** 1978. Ultrastructure and function in sympathetic ganglia isolated from rats infected with pseudorabies virus. Brain Res. **140:**111–123.
18. **Elgadi, M. M., C. E. Hayes, and J. R. Smiley.** 1999. The herpes simplex virus vhs protein induces endoribonucleolytic cleavage of target RNAs in cell extracts. J. Virol. **73:**7153–7164.
19. **Enquist, L. W.** 2002. Exploiting circuit-specific spread of pseudorabies virus in the central nervous system: insights to pathogenesis and circuit tracers. J. Infect. Dis. **186:**S209–S214.
20. **Enquist, L. W., P. J. Husak, B. W. Banfield, and G. A. Smith.** 1998. Infection and spread of alphaherpesviruses in the nervous system. Adv. Virus Res. **51:**237–347.
21. **Enquist, L. W., M. J. Tomishima, S. Gross, and G. A. Smith.** 2002. Directional spread of an alpha-herpesvirus in the nervous system. Vet. Microbiol. **86:**5–16.
22. **Field, H. J., and T. J. Hill.** 1974. The pathogenesis of pseudorabies in mice following peripheral inoculation. J. Gen. Virol. **23:**145–157.
23. **Field, H. J., and T. J. Hill.** 1975. The pathogenesis of pseudorabies in mice: virus replication at the inoculation site and axonal uptake. J. Gen. Virol. **26:**145–148.
24. **Flamand, A., T. Bennardo, N. Babic, B. G. Klupp, and T. C. Mettenleiter.** 2001. The absence of glycoprotein gL, but not gC or gK, severely impairs pseudorabies virus neuroinvasiveness. J. Virol. **75:**11137–11145.
25. **Fraser, G., and S. P. Ramachandran.** 1969. Studies on the virus of Aujeszky's disease. I. Pathogenicity for rats and mice. J. Comp. Pathol. **79:**435–444.
26. **Fuchs, W., H. Granzow, B. G. Klupp, M. Kopp, and T. C. Mettenleiter.** 2002. The UL48 tegument protein of pseudorabies virus is critical for intracytoplasmic assembly of infectious virions. J. Virol. **76:**6729–6742.
27. **Fuchs, W., B. G. Klupp, H. Granzow, C. Hengartner, A. Brack, A. Mundt, L. W. Enquist, and T. C. Mettenleiter.** 2002. Physical interaction between envelope glycoproteins E and M of pseudorabies virus and the major tegument protein UL49. J. Virol. **76:**8208–8217.
28. **Graham, F. L., and A. J. van der Eb.** 1973. A new technique for the assay of infectivity of human adenovirus 5 DNA. Virology **52:**456–467.
29. **Hagemoser, W. A., J. P. Kluge, and H. T. Hill.** 1980. Studies on the pathogenesis of pseudorabies in domestic cats following oral inoculation. Can. J. Comp. Med. **44:**192–202.
30. **Hall, L. B., Jr., J. P. Kluge, L. E. Evans, and H. T. Hill.** 1984. The effect of pseudorabies (Aujeszky's) virus infection on young mature boars and boar fertility. Can. J. Comp. Med. **48:**192–197.
31. **Harper, D. R., and H. O. Kangro.** 1990. Lipoproteins of varicella-zoster virus. J. Gen. Virol. **71:**459–463.

32. **Heffner, S., F. Kovacs, B. G. Klupp, and T. C. Mettenleiter.** 1993. Glycoprotein gp50-negative pseudorabies virus: a novel approach toward a nonspreading live herpesvirus vaccine. J. Virol. **67:**1529–1537.
33. **Hsu, S. M., L. Raine, and H. Fanger.** 1981. Use of avidin-biotin-peroxidase complex (ABC) in immunoperoxidase techniques: a comparison between ABC and unlabeled antibody (PAP) procedures. J. Histochem. Cytochem. **29:**577–580.
34. **Husak, P. J., T. Kuo, and L. W. Enquist.** 2000. Pseudorabies virus membrane proteins gI and gE facilitate anterograde spread of infection in projection-specific neurons in the rat. J. Virol. **74:**10975–10983.
35. **Kaplan, A. S., and A. E. Vatter.** 1959. A comparison of herpes simplex and pseudorabies viruses. Virology **7:**394–407.
36. **Kluge, J. P., and C. J. Mare.** 1974. Swine pseudorabies: abortion, clinical disease, and lesions in pregnant gilts infected with pseudorabies virus (Aujeszky's disease). Am. J. Vet. Res. **35:**991–995.
37. **Klupp, B. G., W. Fuchs, H. Granzow, R. Nixdorf, and T. C. Mettenleiter.** 2002. Pseudorabies virus UL36 tegument protein physically interacts with the UL37 protein. J. Virol. **76:**3065–3071.
38. **Klupp, B. G., H. Granzow, E. Mundt, and T. C. Mettenleiter.** 2001. Pseudorabies virus UL37 gene product is involved in secondary envelopment. J. Virol. **75:**8927–8936.
39. **Kopp, M., H. Granzow, W. Fuchs, B. G. Klupp, E. Mundt, A. Karger, and T. C. Mettenleiter.** 2003. The pseudorabies virus UL11 protein is a virion component involved in secondary envelopment in the cytoplasm. J. Virol. **77:**5339–5351.
40. **Kopp, M., B. G. Klupp, H. Granzow, W. Fuchs, and T. C. Mettenleiter.** 2002. Identification and characterization of the pseudorabies virus tegument proteins UL46 and UL47: role for UL47 in virion morphogenesis in the cytoplasm. J. Virol. **76:**8820–8833.
41. **Lam, Q., C. A. Smibert, K. E. Koop, C. Lavery, J. P. Capone, S. P. Weinheimer, and J. R. Smiley.** 1996. Herpes simplex virus VP16 rescues viral mRNA from destruction by the virion host shutoff function. EMBO J. **15:** 2575–2581.
42. **Loomis, J. S., J. B. Bowzard, R. J. Courtney, and J. W. Wills.** 2001. Intracellular trafficking of the UL11 tegument protein of herpes simplex virus type 1. J. Virol. **75:**12209–12219.
43. **MacLean, C. A., B. Clark, and D. J. McGeoch.** 1989. Gene UL11 of herpes simplex virus type 1 encodes a virion protein which is myristylated. J. Gen. Virol. **70:**3147–3157.
44. **McCabe, J. B., and L. G. Berthiaume.** 1999. Functional roles for fatty acylated amino-terminal domains in subcellular localization. Mol. Biol. Cell **10:**3771–3786.
45. **McCracken, R. M., J. B. McFerran, and C. Dow.** 1973. The neural spread of pseudorabies virus in calves. J. Gen. Virol. **20:**17–28.
46. **McGeoch, D. J., M. S. Dalrymple, A. J. Davison, A. Dolan, M. C. Frame, D. McNab, L. J. Perry, J. E. Scott, and P. Taylor.** 1988. The complete DNA sequence of the unique long region in the genome of herpes simplex virus type 1. J. Gen. Virol. **69:**1531–1574.
47. **McKnight, J. L., P. E. Pellett, F. J. Jenkins, and B. Roizman.** 1987. Characterization and nucleotide sequence of two herpes simplex virus 1 genes whose products modulate alpha-trans-inducing factor-dependent activation of alpha genes. J. Virol. **61:**992–1001.
48. **Mettenleiter, T. C.** 2002. Herpesvirus assembly and egress. J. Virol. **76:**1537–1547.
49. **Mettenleiter, T. C.** 2003. Pathogenesis of neurotropic herpesviruses: role of viral glycoproteins in neuroinvasion and transneuronal spread. Virus Res. **92:**197–206.
50. **Miranda-Saksena, M., R. A. Boadle, P. Armati, and A. L. Cunningham.** 2002. In rat dorsal root ganglion neurons, herpes simplex virus type 1 tegument forms in the cytoplasm of the cell body. J. Virol. **76:**9934–9951.
51. **Mossman, K. L., R. Sherburne, C. Lavery, J. Duncan, and J. R. Smiley.** 2000. Evidence that herpes simplex virus VP16 is required for viral egress downstream of the initial envelopment event. J. Virol. **74:**6287–6299.
52. **Newcomb, W. W., B. L. Trus, F. P. Booy, A. C. Steven, J. S. Wall, and J. C. Brown.** 1993. Structure of the herpes simplex virus capsid: molecular composition of the pentons and the triplexes. J. Mol. Biol. **232:**499–511.
53. **Osorio, F. A., and D. L. Rock.** 1992. A murine model of pseudorabies virus latency. Microb. Pathog. **12:**39–46.
54. **Paxinos, G., and K. B. J. Franklin.** 2000. The mouse brain in stereotaxic coordinates. Academic Press, Inc., San Diego, Calif.
55. **Penfold, M. E., P. Armati, and A. L. Cunningham.** 1994. Axonal transport of herpes simplex virions to epidermal cells: evidence for a specialized mode of virus transport and assembly. Proc. Natl. Acad. Sci. USA **91:**6529–6533.
56. **Ramachandran, S. P., and G. Fraser.** 1971. Studies on the virus of Aujeszky's disease. II. Pathogenicity for chicks. J. Comp. Pathol. **81:**55–62.
57. **Read, G. S., B. M. Karr, and K. Knight.** 1993. Isolation of a herpes simplex virus type 1 mutant with a deletion in the virion host shutoff gene and identification of multiple forms of the vhs (UL41) polypeptide. J. Virol. **67:**7149–7160.
58. **Resh, M. D.** 1999. Fatty acylation of proteins: new insights into membrane targeting of myristoylated and palmitoylated proteins. Biochim. Biophys. Acta **1451:**1–16.
59. **Sanchez, V., E. Sztul, and W. J. Britt.** 2000. Human cytomegalovirus pp28 (UL99) localizes to a cytoplasmic compartment which overlaps the endoplasmic reticulum-Golgi-intermediate compartment. J. Virol. **74:**3842–3851.
60. **Schmidt, S. P., W. A. Hagemoser, J. P. Kluge, and H. T. Hill.** 1987. Pathogenesis of ovine pseudorabies (Aujeszky's disease) following intratracheal inoculation. Can. J. Vet. Res. **51:**326–333.
61. **Smibert, C. A., B. Popova, P. Xiao, J. P. Capone, and J. R. Smiley.** 1994. Herpes simplex virus VP16 forms a complex with the virion host shutoff protein vhs. J. Virol. **68:**2339–2346.
62. **Takahashi, H., Y. Yoshikawa, C. Kai, and K. Yamanouchi.** 1993. Mechanism of pruritus and peracute death in mice induced by pseudorabies virus (PRV) infection. J. Vet. Med. Sci. **55:**913–920.
63. **Tomishima, M. J., and L. W. Enquist.** 2002. In vivo egress of an alphaherpesvirus from axons. J. Virol. **76:**8310–8317.
64. **Yang, M., Card, J. P., Tirabassi, R. S., Miselis, R. R., and L. W. Enquist.** 1999. Retrograde, transneuronal spread of pseudorabies virus in defined neuronal circuitry of the rat brain is facilitated by gE mutations that reduce virulence. J. Virol. **73:**4350–4359.
65. **Zhou, Z. H., D. H. Chen, J. Jakana, F. J. Rixon, and W. Chiu.** 1999. Visualization of tegument-capsid interactions and DNA in intact herpes simplex virus type 1 virions. J. Virol. **73:**3210–3218.
66. **Zhu, Q., and R. J. Courtney.** 1994. Chemical cross-linking of virion envelope and tegument proteins of herpes simplex virus type 1. Virology **204:**590–599.